Int. J. Heat Mass Transfer. Vol. 30, No. 6, pp. 1027–1036, 1987
Printed in Great Britain

0017-9310/87 $3.00 + 0.00
Pergamon Journals Ltd.

Physical model of gradient zone erosion in thermohaline systems

JOHN R. HULL
Argonne National Laboratory, Argonne, IL 60439-4825, U.S.A.

and

JAYESH M. MEHTA†
Department of Mechanical Engineering, Illinois Institute of Technology, 10 W. 32nd St., Chicago, IL 60616, U.S.A.

(*Received* 3 *April* 1986 *and in final form* 9 *September* 1986)

Abstract—A physical model is formulated for gradient zone erosion in thermohaline systems near equilibrium. The model includes the effects at the gradient zone boundaries of temperature modulation, caused by mildly turbulent thermals in adjacent convective zones. The equations that govern convective motion in a double-diffusive horizontal slab are solved for boundary conditions that incorporate these modulations. The result predicts microconvection disturbances within the gradient zone, with an amplitude that decays exponentially away from the boundaries. The expected thickness of observable disturbance is of the order of 1 cm, which agrees with experimental observation. Examining the solution for stability of the boundary yields, for the first time, a model of erosion behavior that agrees with an empirical correlation for boundary equilibrium.

INTRODUCTION

HEAT and mass transfer associated with thermohaline convection is important in a wide range of phenomena [1], including development of saline lakes, melting of icebergs, mixing between ocean layers, freezing and melting of alloys, evolution of stellar interiors, storage and transport of liquid natural gas, and dispersal of sea-discharged effluent. In recent years, there has been growing interest in the use of salt gradient solar ponds for providing space heat, process heat, and power generation. A thermohaline double-diffusive system such as a solar pond usually consists of three zones. The prominent feature is the gradient zone, in which both temperature and salinity increase downward. On the top and bottom of the gradient zone are convective zones of almost homogeneous salinity and temperature. Maintaining the stability of the salt gradient is extremely important for the viable operation of salt gradient solar ponds. Stability within the gradient zone is well understood, both experimentally [2] and theoretically [3], and is unlikely to pose a problem in most practical situations. However, experience at many solar ponds and in laboratory tanks indicates that erosion of the gradient zone at the boundaries is a common occurrence that tends to shrink the thickness of the gradient zone to a value significantly smaller than that required for thermal optimization [4]. A typical range of heat flux through the bottom of the solar pond gradient zone is of the order of 5–50 $W m^{-2}$, although it may be as high as 400 $W m^{-2}$ at the top.

To date no fundamental understanding exists for the erosion phenomenon, although many models describe some aspects of the erosion behavior. The best description is given by the Nielsen equilibrium criterion [4, 5], an empirical relation that describes conditions for growth and shrinkage in NaCl thermohaline systems. The criterion relates the temperature gradient and the salt gradient at the gradient zone boundary in the absence of external disturbances according to

$$dT/dy = A(dS/dy)^{1.6} \quad (1)$$

where $A = 5 \times 10^{-3}\,K\,m^{5.4}\,kg^{-1.6}$. When dT/dy is larger than the right-hand side of equation (1), the gradient zone erodes. When dT/dy is less than the right-hand side, the gradient zone grows into the convective zone.

Past efforts to understand the erosion behavior have used many empirical correlations and at best give an incomplete picture of the behavior. Meyer [6] proposed a one-dimensional model based on an empirical correlation between salt and heat flux for thin diffusive interfaces [7]. In this model thermal and salinity boundary layers diffuse outward from the diffusive core of the gradient zone at different rates until the thermal boundary layer becomes unstable. At this point the model assumes that both boundary layers are fully mixed into the convective zone at breakdown. Bergman *et al.* [8] developed a one-

† Current address: General Electric Co., Combustion and Heat Transfer Technology, Mail Zone K64, 1 Neumann Drive, Evendale, OH 45215, U.S.A.

NOMENCLATURE

A	empirical constant [K m$^{5.4}$ kg$^{-1.6}$]
A_1	stability constant, $vk_TR_e/(g\alpha)$ [K m^3]
A_2	stability constant
A_3	stability constant
a_0	temperature modulation [K]
B_1, B_2, B_4, B_5	proportionality constants
B_3	empirical constant [9.74 m$^{-1/2}$ W$^{-1/4}$]
c	empirical constant
D	lower convective zone thickness [m]
d	gradient zone thickness [m]
E_b	energy in individual thermal burst [J]
g	acceleration of gravity [m s^{-2}]
H	heat flux [W m^{-2}]
K	thermal conductivity [W m^{-1} K^{-1}]
k	modulation wave number [m^{-1}]
k_S	solutal diffusivity [m^2 s^{-1}]
k_T	thermal diffusivity [m^2 s^{-1}]
L_e	critical length for erosion [m]
L_T	thermal diffusion length [m]
L_1	critical length ratio, $L_ep^{1/2}$
Nu	Nusselt number for lower convective zone, $HD/(K\delta T)$
p	solution parameter, $(k^2g\beta(dS_0/dy)(1-\gamma)/(vk_S))^{1/3}$ [m^{-2}]
Pr	Prandtl number
Ra	Rayleigh number for lower convective zone, $g\alpha D^3\delta T/(vk_T)$
R_e	critical Rayleigh number for erosion, $g\alpha L_e^4(dT/dy)/(vk_T)$
R_S	solutal Rayleigh number for gradient zone, $-g\beta d^4(dS_0/dy)/(vk_T)$
R_T	thermal Rayleigh number for gradient zone, $-g\alpha d^4(dT_0/dy)/(vk_T)$
R_δ	critical Rayleigh number for thermal boundary layer, $g\alpha\delta^3\delta T/(vk_T)$
R_ρ	density stability ratio for gradient zone, R_S/R_T
S	salinity [kg m^{-3}]
ΔS	salinity difference across gradient zone [kg m^{-3}]
$s(y)$	vertical dependence of salinity
s_i	salinity coefficient, $i = 1, 2, 3, 4$
T	temperature [K]
ΔT	temperature difference across gradient zone [K]
$t(y)$	vertical dependence of temperature
t_i	temperature coefficient, $i = 1, 2, 3, 4$
t_b	time between thermal bursts [s]
t_c	critical time of thermal, traveling in lower convective zone [s]
$\bar{t}$	time of travel for thermal, t/t_c
v	vertical velocity of thermal [m s^{-1}]
v_c	critical velocity of thermal [m s^{-1}]
$\bar{v}$	vertical velocity of thermal, v/v_c
x	horizontal spatial coordinate [m]
y	vertical spatial coordinate positive upwards [m].

Greek symbols

α	thermal expansion coefficient, $-(1/\rho)(\partial\rho/\partial T)$ [K^{-1}]
β	salinity expansion coefficient, $(1/\rho)(\partial\rho/\partial S)$ [m^3 kg^{-1}]
γ	diffusive stability ratio, τ/R_ρ
$\bar{\Delta}$	temperature difference between thermal burst and lower convective zone, $a_0/\delta T$
δ	thermal boundary layer thickness [m]
δT	temperature difference across thermal boundary layer [K]
ε	dimensionless temperature modulation, $a_0/\Delta T$
λ_i	eigenvalue, $i = 1, 2, 3, 4$ [m^{-1}]
ν	kinematic viscosity [m^2 s^{-1}]
ρ	density [kg m^{-3}]
τ	ratio of diffusivities, k_S/k_T
$\phi(y)$	vertical dependence of stream function
ϕ_i	stream function coefficient, $i = 1, 2, 3, 4$
Ψ	stream function [m^2 s^{-1}].

Subscripts

0	zeroth-order solution
1	first-order solution.

Superscripts

n	empirical coefficient
n_1	stability criterion coefficient, $(6n+2)/(9n+9)$
n_2	stability criterion coefficient, $-(3n+1)/(6n+6)$.

dimensional multi-layer model by applying species and energy balances to control volumes about the bottom convective zone and the gradient zone. Gradient zone erosion was represented by an entrainment velocity correlated to the friction velocity associated with turbulence in the convective zone and a bulk Richardson number based on a density jump at the zone boundary. This model was later developed into a differential model that incorporated a k–ε model of turbulent entrainment [9]. Atkinson and Harleman [10] have also suggested a one-dimensional erosion model based on a correlation of entrainment of turbulent kinetic energy.

Newell [11] characterized the dynamics of thin gradient zones according to the density stability ratio R_ρ. Witte and Newell [12] used a thermal burst stability model as the basis for erosion/growth rate predictions. In this case diffusion at the gradient zone boundary is the governing physical mechanism, and the influence of fluid behavior in the convective zone is ignored.

A number of laboratory experiments have used shadowgraph [13, 14], Mach–Zehnder interferometer [15], and color dye flow visualization [16], as well as salinity and temperature measurements [11, 17, 18], to elucidate some of the details of fluid motion during the erosion process. Fluid flow in the bottom convective zone is characterized by mildly turbulent convection, consisting of thermals rising from the heated bottom and descending from the gradient zone boundary. The thermals themselves are randomly driven laminar flows that break off from a thermal boundary layer, with each individual thermal persisting for many minutes [15, 17]. With a bottom heating rate from 40–90 W m^{-2}, the 1–2 cm diameter thermals [17] have a velocity of the order of 1–2 mm s^{-1} [16], a horizontal spacing of 3–6 cm [16], and a temperature difference with the background of 0.1–0.2 K [17]. When a rising thermal impinges on the zone boundary, it may cause a local deflection of 1 mm or more [14, 15].

Seen by shadowgraph [13, 14], a boundary layer of 5–30 mm thickness separates the diffusive core of the gradient zone from the adjacent convective zone. At a given horizontal location in a system near equilibrium, the temperature boundary often extends into the convective zone past the salinity boundary by about 1 cm [11, 17, 18]. While the salinity boundary remains relatively fixed in time, the apparent vertical position of the temperature boundary will experience fluctuations of the order of 1 cm with a period of the order of minutes [17]. At a fixed position near the average boundary position, temperature fluctuations of about 0.2 K are observed, whereas at a fixed position several centimeters into the gradient zone, temperature fluctuations are less than 0.001 K [17].

The one-dimensional models [6, 8–12] often give reasonable results under conditions where the erosion rate is rapid but do less well under conditions closer to equilibrium. Only one model [12] has tried to predict growth of the gradient zone. No model has been able to predict the equilibrium criterion of equation (1). No model has been able to explain the thickness of the boundary layer or explain the observed temperature fluctuations. Accordingly, in the present study we have formulated a model that is capable of predicting the thickness of the boundary layer, the behavior of the temperature fluctuations, and the conditions for which equilibrium against erosion or growth exist, in good agreement with experimental observations. The present work uses thermal conditions that result from the fluid motions in the convective zone as boundary conditions for deriving two-dimensional flow in the gradient zone.

GRADIENT ZONE MODEL

This paper studies the erosion problem from an analytical perspective, using the Navier–Stokes equations and stability theory as a basis. The analysis assumes that convective thermals in the adjoining convective zone produce a spatially varying temperature distribution along the gradient zone boundary that is constant for a period of time that is long compared with the time scale for motion within the gradient zone. The salinity at the boundary is assumed constant and the boundary is dynamically free. The model assumes that both the temperature and salinity boundaries are at the same vertical coordinate, greatly simplifying the analysis. While this assumption conflicts somewhat with observation [11, 17, 18], the simplification is warranted because the goal here is to investigate the effect of the temperature modulations. A previous analysis of this type has examined the effect of temperature boundary modulations on one-component thermal systems [19]. In this paper we discuss the effects of temperature modulation at the lower boundary only. The generalization to the case with modulations at both boundaries is straightforward [20], and for the most part, modulation at one boundary does not affect fluid flow near the other boundary.

As shown in Fig. 1, a horizontal fluid slab is bounded by two stress-free boundaries at $y = 0$ and d. The salinity and temperature at both boundaries are constant in time with

$$S = 0, \quad T = 0, \quad \text{at } y = d$$
$$S = \Delta S, \quad T = \Delta T + a_0 \sin kx, \quad \text{at } y = 0$$

where

$$\varepsilon = a_0/\Delta T \ll 1.$$

We assume that the fluid is incompressible, the Boussinesq approximation is valid, the thermophysical properties are constant, density increases linearly with salinity and decreases linearly with temperature, and the Soret and Dufour effects can be ignored. With gravity acting in the negative y-

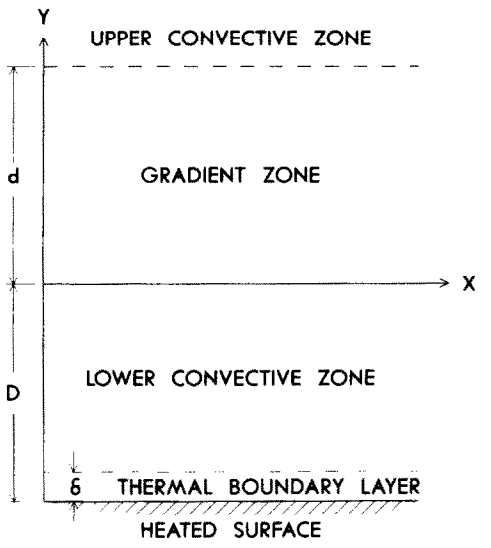

FIG. 1. Schematic of thermohaline system.

direction, for a two-dimensional convection, the steady-state conservation equations are

$$k_S \nabla^2 S = \frac{\partial \Psi}{\partial y}\frac{\partial S}{\partial x} - \frac{\partial \Psi}{\partial x}\frac{\partial S}{\partial y} \tag{2}$$

$$k_T \nabla^2 T = \frac{\partial \Psi}{\partial y}\frac{\partial T}{\partial x} - \frac{\partial \Psi}{\partial x}\frac{\partial T}{\partial y} \tag{3}$$

$$\nabla^4 \Psi + \frac{g\beta}{\nu}\frac{\partial S}{\partial x} - \frac{g\alpha}{\nu}\frac{\partial T}{\partial x} = \frac{1}{\nu}\left[\frac{\partial \Psi}{\partial y}\left(\frac{\partial^3 \Psi}{\partial x \partial y^2} + \frac{\partial^3 \Psi}{\partial x^3}\right) - \frac{\partial \Psi}{\partial x}\left(\frac{\partial^3 \Psi}{\partial y^3} + \frac{\partial^3 \Psi}{\partial y \partial x^2}\right)\right]. \tag{4}$$

To make the equations compatible we nondimensionalize the variables according to

$$x^* = x/d, \quad y^* = y/d, \quad T^* = T/\Delta T, \quad S^* = S/\Delta S,$$
$$\Psi^* = \Psi/k_T, \quad k^* = kd, \quad p^* = pd^2$$

where the starred variables are nondimensional. For brevity the asterisk is omitted in the analysis that follows. The non-dimensionalized boundary conditions are

$$S = 0,\ T = 0, \qquad \Psi = 0,\ \partial^2\Psi/\partial y^2 = 0, \text{ at } y = 1$$
$$S = 1,\ T = 1 + \varepsilon \sin kx, \qquad \Psi = 0,\ \partial^2\Psi/\partial y^2 = 0, \text{ at } y = 0.$$

Writing the variables as an expansion in ε

$$(S, T, \Psi) = \sum_{n=0}^{\infty} \varepsilon^n (S_n, T_n, \Psi_n) \tag{5}$$

the equations to zeroth order in ε yield the solution with no temperature modulation

$$S_0(x, y) = 1 - y, \quad T_0(x, y) = 1 - y, \quad \Psi_0(x, y) = 0. \tag{6}$$

The equations to first order in ε are

$$\tau \nabla^2 S_1 = \partial \Psi_1/\partial x \tag{7}$$

$$\nabla^2 T_1 = \partial \Psi_1/\partial x \tag{8}$$

$$\nabla^4 \Psi_1 + R_S \partial S_1/\partial x - R_T \partial T_1/\partial x = 0. \tag{9}$$

Note that k_T, not k_S, appears in the denominator in the definition of R_S. The boundary conditions for equations (7)–(9) are

$$S_1 = 0, T_1 = 0, \qquad \Psi_1 = 0, \partial^2\Psi_1/\partial y^2 = 0, \text{at } y = 1$$
$$S_1 = 0, T_1 = \sin kx, \Psi_1 = 0, \partial^2\Psi_1/\partial y^2 = 0, \text{at } y = 0.$$

We assume solutions of the form

$$S_1(x, y) = s(y) \sin kx \tag{10}$$

$$T_1(x, y) = t(y) \sin kx \tag{11}$$

$$\Psi_1(x, y) = \phi(y) \cos kx \tag{12}$$

where

$$s(y) = \sum_{i=1}^{4} s_i \frac{\sinh \lambda_i (1 - y)}{\sinh \lambda_i} \tag{13}$$

$$t(y) = \sum_{i=1}^{4} t_i \frac{\sinh \lambda_i (1 - y)}{\sinh \lambda_i} \tag{14}$$

$$\phi(y) = \sum_{i=1}^{4} \phi_i \frac{\sinh \lambda_i (1 - y)}{\sinh \lambda_i}. \tag{15}$$

The solution for the eigenvalues is

$$\lambda_1 = k, \quad \lambda_2 = (p + k^2)^{1/2},$$
$$\lambda_3 = [p \exp(i\, 2\pi/3) + k^2]^{1/2},$$
$$\lambda_4 = [p \exp(i\, 4\pi/3) + k^2]^{1/2} \tag{16}$$

where

$$p = [k^2 R_T (1 - \gamma)/\gamma]^{1/3} \tag{17}$$

and the square root is evaluated so that λ_3 and λ_4 are complex conjugates. For typical parameter values of interest, $k^2 \ll p$, and the real parts of λ_3 and λ_4 are approximately half the value of λ_2. The solution for the coefficients is

$$s_1 = \frac{1}{R_\rho(1 - \gamma)}, \quad s_2 = s_3 = s_4 = -\frac{1}{3R_\rho(1 - \gamma)} \tag{18}$$

$$t_1 = \frac{1}{1 - \gamma}, \quad t_2 = t_3 = t_4 = -\frac{\gamma}{3(1 - \gamma)} \tag{19}$$

$$\phi_1 = 0, \qquad \phi_2 = \frac{\gamma p}{3k(1 - \gamma)}$$
$$\phi_3 = \frac{\gamma p \exp(i\, 2\pi/3)}{3k(1 - \gamma)}, \quad \phi_4 = \frac{\gamma p \exp(i\, 4\pi/3)}{3k(1 - \gamma)}. \tag{20}$$

CONVECTIVE ZONE MODEL

In order to determine k and a_0, we need to specify the properties of the thermals and the convective motion in the lower convective zone. The depth of the convective zone may be 10 cm or more for laboratory experiments and may be 1.0 m or more in a solar pond. The bottom of the convective zone is heated uniformly and develops a thermal boundary layer from which the thermals originate. Heat transfer in the convective zone is given by the correlation

$$Nu = c\,Ra^n \tag{21}$$

where n is often taken as 1/3, but experimental results for large Rayleigh numbers ($Ra > 10^5$) have varied from $n = 0.278$ to 0.33 [21–24]. Using equation (21) and the definitions of Nu and Ra, we derive

$$\delta T = B_1 H^{1/(n+1)}. \tag{22}$$

Taking $n = 1/3$ and $c = 0.076$ [24], for $D = 10$ cm, $Ra = 5.4 \times 10^6$ for $H = 10\,\mathrm{W\,m^{-2}}$, and $Ra = 1.5 \times 10^7$ for $H = 40\,\mathrm{W\,m^{-2}}$. These Rayleigh numbers correspond to turbulent convection. In the solar pond at $D = 1.0$ m, the Rayleigh numbers are higher by a factor of 1000, however the solar pond is not totally heated from below. The heat input to the solar pond is derived from solar radiation absorbed mostly on the bottom, but partly within the lower convective zone. The absorption within the water causes a partial thermal stratification, which will tend to slow the rise of the thermals and make the convection correspond more with the laboratory experiments.

The turbulent convection regime can be described by the thermal burst model of Howard [25], which gives good agreement with many features of the thermals that have been observed experimentally [26]. In the thermal burst model the thermal boundary layer at the bottom of the convective zone starts from an initially isothermal fluid at the mean temperature of the convective zone and develops by diffusion until the Rayleigh number defined over the boundary layer reaches R_δ. At this point a segment of the boundary layer breaks off as a thermal burst and rises by buoyancy force, with fluid from above the boundary layer taking its place to repeat the cycle. Observations [26] indicate that the thermals originate at locations spaced uniformly along the bottom. Once established, the locations last for long periods of time with bursts repeatedly rising from the same location. Successive thermals may meander in their path through the convective zone and impinge the gradient zone at different locations.

The horizontal wavelength of the disturbance within the boundary layer is proportional to δ [24], and thus the energy in each thermal burst is given by

$$E_b = B_2 \delta^3 \delta T. \tag{23}$$

From the definition of R_δ, $\delta^3 \delta T$ is a constant, and therefore the energy in each thermal burst is constant, independent of the heat flux. The heat flux is given by

$$H = E_b k^2 / t_b. \tag{24}$$

The time t_b is proportional to the diffusion time [26], which is proportional to δ^2. We relate the thickness δ to H by equation (22) and the definition of R_δ and substitute the result into equation (24) to obtain

$$k = B_3 H^{(3n+1)/(6n+6)}. \tag{25}$$

For $n = 1/3$, k is proportional to $H^{1/4}$.

The evolution of the thermal burst in its passage through the convective zone has been analyzed by Escudier and Maxworthy [27]. Applying their analysis to the convective zone size and heat flux range considered in this study, one can show that the acceleration phase of the thermal occupies a small fraction of the total distance traveled, and that the behavior of the thermal may be described by the long time limit. In this limit the temperature and velocity of the thermal are described by (setting the impulse parameter to 0.25) [27]

$$\bar{\Delta} = 0.6\,\bar{t}^{-3/2} \tag{26}$$

$$\bar{v} = 0.56\bar{t}^{-1/2}. \tag{27}$$

By ignoring the distance traveled in the acceleration phase, we derive the value for $\bar{t}$ from

$$D = \int_0^t v\,dt \tag{28}$$

and because $v_c t_c$ is proportional to δ [27], we obtain

$$\bar{t} = B_4 D^2 / \delta^2. \tag{29}$$

Substituting equation (29) in equation (26), we obtain

$$a_0 = B_5 \delta^3 \delta T / D^3. \tag{30}$$

Because $\delta^3 \delta T$ is constant, a_0 is constant, independent of H.

DISCUSSION

Using the theoretical results of the previous sections, we examine the temperature and salinity distributions and the fluid flow in the gradient zone for conditions typical of solar ponds and some of the laboratory experiments. The thermophysical properties are those for an NaCl solution of $S = 106\,\mathrm{kg\,m^{-3}}$ (10% by weight) and $T = 50°C$: $\nu = 6.2 \times 10^{-7}\,\mathrm{m^2\,s^{-1}}$, $k_S = 2.6 \times 10^{-9}\,\mathrm{m^2\,s^{-1}}$, $k_T = 1.6 \times 10^{-7}\,\mathrm{m^2\,s^{-1}}$, $\alpha = 4.6 \times 10^{-4}\,\mathrm{K^{-1}}$, $\beta = 6.2 \times 10^{-4}\,\mathrm{m^3\,kg^{-1}}$, $Pr = 4.0$, $K = 0.63\,\mathrm{W\,m^{-1}\,K^{-1}}$. From Kamal and Nielsen [17] we assume $k = 24.5\,\mathrm{m^{-1}}$ at $H = 40\,\mathrm{W\,m^{-2}}$ and $a_0 = 0.2$ K, independent of H. We also assume $n = 1/3$ in equations (22) and (25). The heat flux

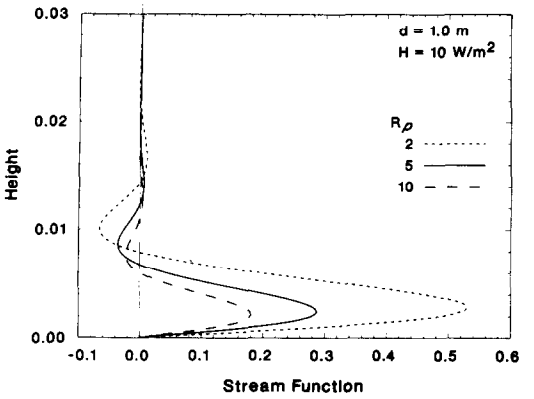

FIG. 2. Calculated stream function distribution for several R_ρ at $H = 10\,\mathrm{W\,m^{-2}}$.

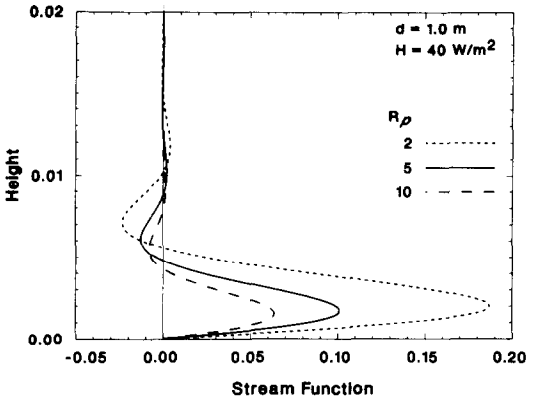

FIG. 3. Calculated stream function distribution for several R_ρ at $H = 40\,\mathrm{W\,m^{-2}}$.

is related to the temperature gradient in the gradient zone according to

$$H = -K\,\mathrm{d}T_0/\mathrm{d}y. \tag{31}$$

One effect of the temperature modulation is the creation of a small mean flow in what otherwise would be a quiescent fluid. We designate this flow as microconvection to distinguish it from the large-scale motions occurring in the convective zone. Distributions of the stream function $\phi(y)$ are shown in Figs. 2 and 3, at a heat flux of 10 and 40 $\mathrm{W\,m^{-2}}$, respectively, for several R_ρ at a gradient zone thickness of $d = 1.0\,\mathrm{m}$. The amplitude of the stream function dies off exponentially away from the boundary with an attenuation length $2p^{-1/2}$. In the first microconvection cell at the bottom of the gradient zone, the flow is upwards above the center of the impinging thermal ($\sin kx = 1$). This is expected as the increase in temperature at the boundary at this location gives the adjacent gradient zone fluid positive buoyancy. Because of the horizontal variation in heating at the zone boundary, the microconvection should commence shortly after the thermal arrives to set up the temperature boundary.

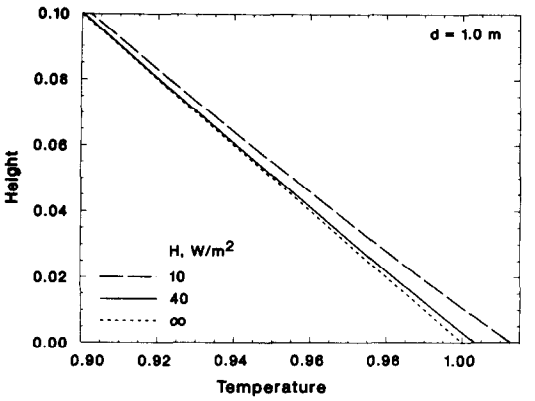

FIG. 4. Calculated temperature distribution for several heat fluxes.

The magnitude of the velocity is larger and the penetration into the gradient zone greater for smaller values of both H and R_ρ. When the calculations are performed at $d = 0.1\,\mathrm{m}$, the values for the stream function are essentially identical for a given H and R_ρ when plotted against the dimensioned y-coordinate. This shows that the convective motion is dependent only on the salinity and temperature gradients and lends support to the earlier statement that modulations at one boundary do not affect the flow near the other boundary. As indicated in Figs. 2 and 3, the microconvection exists only in the bottom 1–2 cm of the gradient zone. The actual velocities are relatively small, with the larger velocities occurring at the lower heat fluxes. At $H = 10\,\mathrm{W\,m^{-2}}$ and $R_\rho = 2$, the maximum horizontal velocity is $4.0 \times 10^{-5}\,\mathrm{m\,s^{-1}}$, and the maximum vertical velocity is $1.5 \times 10^{-6}\,\mathrm{m\,s^{-1}}$.

The steady-state temperature distribution $T(y) = T_0 + \varepsilon t(y)$ for several heat fluxes is shown in Fig. 4. An infinite heat flux is equivalent to the base state of no modulation. The temperature distribution is essentially independent of R_ρ. The function $t(y)$ is mainly governed by the t_1 term, in which the amplitude dies off exponentially with attenuation length $1/k$, characteristic of diffusion. The other three terms have the much shorter decay length of the order of $p^{-1/2}$, which is a characteristic length of the microconvection. However, compared to the diffusive term, the amplitude for the three convective terms is reduced by the factor γ, which is of the order of 0.01 or less, and these terms play a negligible role in the temperature distribution.

The steady-state temperature distribution thus arises mainly from thermal diffusion from the boundary. If the position of the thermals at the gradient zone boundary were indeed constant in time, one would expect to be able to detect a horizontal temperature variation well into the diffusive core of the gradient zone. Such variations have not been detected [17]. The thermal diffusion length is given by

$$L_T = (2k_T t)^{1/2} \tag{32}$$

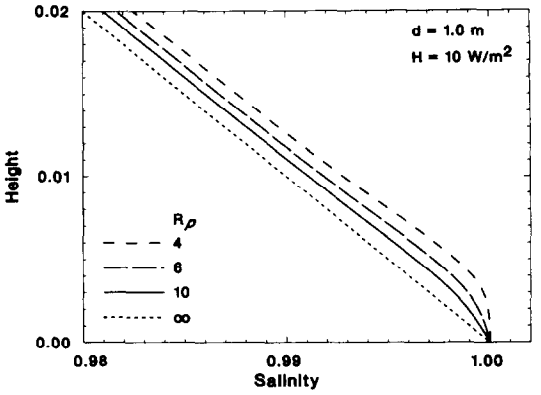

FIG. 5. Calculated salinity distribution for several R_ρ at $H = 10\,\mathrm{W\,m^{-2}}$.

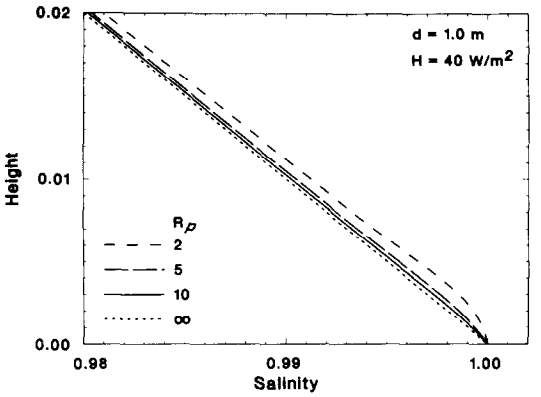

FIG. 6. Calculated salinity distribution for several R_ρ at $H = 40\,\mathrm{W\,m^{-2}}$.

and because of the randomly driven nature of the thermals, one does not expect to see a temperature variation into the gradient zone much beyond this length. For a coherence period for the thermals of $t = 1000\,\mathrm{s}$ [26], $L_T = 1.8\,\mathrm{cm}$. Thus one would not expect to see temperature fluctuations much beyond the region of microconvection, in agreement with observation [17].

The salinity distribution $S(y) = S_0 + \varepsilon s(y)$ for the heat fluxes 10 and $40\,\mathrm{W\,m^{-2}}$ are shown in Figs. 5 and 6, respectively, for several values of R_ρ. An infinite R_ρ is equivalent to the base state of no modulation. Near the boundary, the solution for $s(y)$ needs a second-order correction for low H and R_ρ (e.g. $H = 10\,\mathrm{W\,m^{-2}}$, $R_\rho = 2$), but this parameter region is not in the area where boundary equilibrium is attained, and we ignore the correction in further discussion.

As was the case for temperature, the s_1 diffusion term in $s(y)$ decays with length $1/k$, while the other three convective terms decay with length of the order $p^{-1/2}$. Unlike temperature, however, all the salinity coefficients are approximately the same magnitude, and there is a significant salinity variation from the base state within the lowest microconvection cell. The salinity gradient becomes very weak above the impinging thermal. At this location the salinity gradient decreases with both decreasing H and R_ρ. Physically, salt from near the boundary is convected upward by the microconvection. At the same time, lower salinity solution is convected downward in the lowest cell at the horizontal location between the thermals, forming a stronger salinity gradient in these locations. Because the solutal diffusivity is small, these salinity distributions are likely to persist after a thermal changes location.

The above discussion indicates that non-linear salinity and density distributions are expected to occur within the region of microconvection. Temperature fluctuations within the gradient zone are also expected to be confined mainly within this microconvection region. Thus, a key prediction of the theory is the depth of the microdisturbances within the gradient zone at the zone boundary. For conditions typical of a solar pond, the vertical convection wavelength is of the order of 1 cm. This predicted depth appears to agree with experimental observations [14, 16–18].

BOUNDARY EROSION

Given the results of the previous sections, the base state temperature and salinity profiles in the gradient zone can be used to predict the stability of the fluid at the gradient zone boundary, i.e. to derive a relation that corresponds to the Nielsen equilibrium criterion. As indicated in Figs. 5 and 6, in the bottom of the gradient zone immediately above an impinging thermal, the salinity gradient becomes very weak, and in some cases disappears completely over a height of several millimeters. We use this observation as a basis for formulating a simple model of gradient zone erosion. We assume a negligible salinity gradient over some critical length L_e at the bottom of the gradient zone, which defines the vertical height of a potential erosion cell. When erosion occurs, the temperature gradient and L_e have become sufficiently large so that the thermal Rayleigh number defined over L_e is larger than some critical value R_e. At this point instability and convection will occur, and we assume that the convecting fluid eventually mixes with the lower convective zone. The effect of the erosive convection is to transport colder fluid from the top of the convection cell to the gradient zone boundary. This colder fluid has the same salinity as the convective zone and forms a descending thermal. The net effect is the entrainment of gradient zone fluid into the lower convective zone.

Because the velocity of the microconvection is so small, we assume that stability theory of quiescent fluids applies here. It is not clear what value should be used for R_e. There is convection occurring on both sides of the potential erosion cell, which suggests constant temperature boundaries and $R_e = 657$. On the other hand, the upper boundary is dominated by

the initial temperature gradient, which suggests a constant heat flux boundary for which $R_e = 385$ [28]. There is also some uncertainty regarding the proper choice for L_e. We assume that L_e is related to the microconvection wavelength according to

$$L_e = L_1/p^{1/2}. \tag{33}$$

The region of weak salinity gradient is within the lowest cell of the microconvection, and we thus expect $L_1 < 2\pi/3^{1/2}$. The horizontal wavelength of the erosive convection is of the same order as L_e [28], which is well within the $1/k$ width of the modulation.

While the Soret effect is usually important in determining convective instability at these length scales [29], it is not likely to be important in this problem. In a two-component system heated from below, a major influence of the Soret effect is to change the salinity distribution, which in our case manifests itself in a change in the base state value for R_S.

Combining equation (33) with the definition of R_e, the required temperature gradient to cause erosion is given by

$$\mathrm{d}T/\mathrm{d}y = A_1 p^2/L_1^4. \tag{34}$$

The temperature gradient across L_e is equal to the original gradient plus an additional gradient caused by the temperature profile developing by diffusion caused by the presence of the thermal. Erosion may occur only after the thermal diffusion length equals L_e, thus the temperature gradient is given by

$$\mathrm{d}T/\mathrm{d}y = \mathrm{d}T_0/\mathrm{d}y + a_0/L_e. \tag{35}$$

For equation (35) to be valid, it is necessary that the thermal diffusion time approximately equal or exceed the time it takes to transport salt a vertical distance L_e by the microconvection in the first cell. This result holds for the parameter range of interest. We use equations (25), (31), (33), and (34) in equation (35) to obtain the condition for marginal stability

$$A_2(\mathrm{d}S_0/\mathrm{d}y)^{2/3} = (\mathrm{d}T_0/\mathrm{d}y)^{n_1} + A_3(\mathrm{d}S_0/\mathrm{d}y)^{1/6}(\mathrm{d}T_0/\mathrm{d}y)^{n_2} \tag{36}$$

where

$$n_1 = (3n + 7)/(9n + 9) \tag{37}$$

$$n_2 = -(3n + 1)/(6n + 6) \tag{38}$$

$$A_2 = \nu^{1/3} k_T R_e B_3^{4/3} K^{(6n+2)/(9n+9)} \times \beta^{2/3} g^{-1/3} \alpha^{-1} k_S^{-2/3} L_1^{-4} \tag{39}$$

$$A_3 = a_0 B_3^{1/3} g^{1/6} \beta^{1/6} K^{(3n+1)/(18n+18)} \times \nu^{-1/6} K_S^{-1/6} L_1^{-1} \tag{40}$$

$$B_3 = (24.5)(40)^{n_2}. \tag{41}$$

For a given $\mathrm{d}T_0/\mathrm{d}y$, equation (36) is readily solved by iteration for $\mathrm{d}S_0/\mathrm{d}y$.

Lines of marginal stability for several theories of thermohaline systems are shown in Fig. 7 over a range of $H = 6$–$400\ \mathrm{W\,m^{-2}}$ for thermophysical properties equivalent to $T = 50°\mathrm{C}$, $S = 106\ \mathrm{kg\,m^{-3}}$, and $n = 1/3$. Predicted instability occurs for parameter values above the marginal lines. The classical line of marginal stability theory, given by

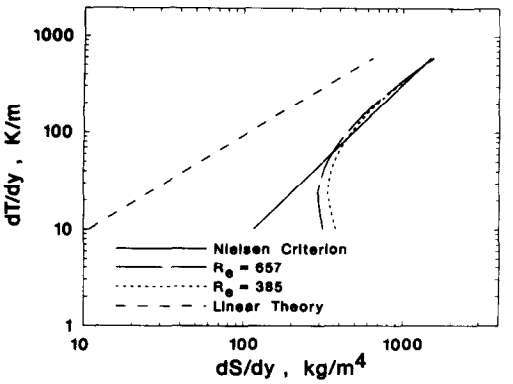

FIG. 7. Temperature gradient as a function of salinity gradient for lines of marginal stability, comparing present theory with Nielsen criterion and linear stability theory.

$$\mathrm{d}T_0/\mathrm{d}y = [(Pr + \tau)/(Pr + 1)](\beta/\alpha)(\mathrm{d}S_0/\mathrm{d}y) \tag{42}$$

for large R_T ($d > 10\,\mathrm{cm}$) applies to a vertical segment anywhere within the gradient zone [2, 3]. The other three lines apply only at the gradient zone boundary and indicate that boundary erosion will occur for conditions where the gradient zone interior is very stable ($R_\rho = 3$–12). The solution to equation (36) is shown in Fig. 7 for $R_e = 385$ and 657. For these two lines the value of L_1 has been varied to yield the best fit to the Nielsen criterion of equation (1). The best fit values for L_1 are $L_1 = 3.18$ for $R_e = 657$, and $L_1 = 2.77$ for $R_e = 385$. These values yield 88 and 76% of the lower cell thickness, respectively, which is in the expected range. When n is varied between 0.28 and 0.34, there is no significant difference in L_1, goodness of fit, or position of the two lines. As seen in Fig. 7, there is good agreement between the present theory and the Nielsen criterion at most of the heat fluxes ($H > 20\ \mathrm{W\,m^{-2}}$). The largest percentage discrepancy occurs at the lowest H. This is the region where uncertainty in $\mathrm{d}T_0/\mathrm{d}y$ for the Nielsen criterion is largest because the temperature difference across a typical experimental gradient zone is then small.

The erosive convection could never develop if the characteristic time for the microconvection and development of the enhanced temperature gradient in the gradient zone were longer than the time between thermal bursts. Because L_e is generally less than δ, and the characteristic times are those of thermal diffusion, this is not the case.

CONCLUSIONS

We have formulated a physical model of gradient zone erosion in thermohaline systems near equilibrium. Regularly spaced thermals in the adjacent

convective zone cause temperature modulation at the gradient zone boundary. The temperature modulation drives microconvection cells in the lower portion of the gradient zone. Erosion occurs when the salinity gradient in the lowest microconvection cell above an impinging thermal becomes too weak to support the temperature gradient. The conditions for marginal stability of the erosion process are given by equation (36).

The theoretical predictions for thickness of the microconvection and the temperature distribution within the gradient zone agree well with experimental observation. The theoretical prediction for equilibrium conditions governing erosion and growth of the gradient zone is in good agreement with a long existing empirical correlation, equation (1), for this behavior. To our knowledge this is the first time that any theory has been capable of predicting these equilibrium conditions.

The agreement between the present theory and the correlation of equation (1) is somewhat remarkable in view of the simplifications made in the theory. The theory does not incorporate spatial indentations of the boundary caused by the momentum of the thermal. The effect of these indentations is expected to become more important at lower heat flux values, because the density gradient then provides a weaker restoring force while the buoyancy of each thermal is mostly independent of heat flux. The theory also does not incorporate diffusion of the gradient zone into the convective zone nor the observation that the temperature boundary of the gradient zone has a slightly different vertical coordinate than the salinity boundary. The theory of erosion is very simplistic, assuming the microconvection velocity does not affect stability, ignoring details of the temperature and salinity distributions, and also making no attempt to describe the fluid motion after erosive instability sets in. These effects must be incorporated into any complete description of gradient zone erosion.

Acknowledgements—This work was partly sponsored by the U.S. Department of Energy under Contract W-31-109-Eng-38. Parts of this work were submitted by the second author towards fulfillment of the requirements for a Ph.D. degree. He would like to thank Drs S. Rosenblat and S. Nair, of IIT, for many stimulating discussions during the course of this study.

REFERENCES

1. H. E. Huppert and J. S. Turner, Double-diffusive convection, *J. Fluid Mech.* **106,** 299–329 (1981).
2. F. Zangrando and L. A. Bertram, The effect of variable stratification on linear doubly diffusive stability, *J. Fluid Mech.* **151,** 55–79 (1985).
3. I. C. Walton, Double-diffusive convection with large variable gradients, *J. Fluid Mech.* **125,** 123–135 (1982).
4. J. R. Hull, Y. S. Cha, W. T. Sha and W. W. Schertz, Construction and first year's operational results of the ANL research salt gradient solar pond, *Proc. Am. Solar Energy Soc.*, pp. 197–202, Houston (1982).
5. C. E. Nielsen, Control of gradient zone behavior, *Proc. Int. Solar Energy Soc.*, pp. 1010–1014, Atlanta (1979).
6. K. A. Meyer, A numerical model to describe the layer behavior in salt gradient solar ponds, *ASME J. Solar Energy Engng* **105,** 341–347 (1983).
7. J. S. Turner, The coupled turbulent transports of salt and heat across a sharp density interface, *Int. J. Heat Mass Transfer* **8,** 759–767 (1965).
8. T. L. Bergman, F. P. Incropera and R. Viskanta, A multi layered model for mixing layer development in a double-diffusive thermohaline system heated from below, *Int. J. Heat Mass Transfer* **25,** 1411–1418 (1982).
9. T. L. Bergman, F. P. Incropera and R. Viskanta, A differential model for salt-stratified double-diffusive systems heated from below, *Int. J. Heat Mass Transfer* **28,** 779–788 (1985).
10. J. F. Atkinson and D. R. F. Harleman, A wind-mixed layer model for solar ponds, *Solar Energy* **31,** 243–259 (1983).
11. T. A. Newell, Characteristics of a double-diffusive interface at high density stability ratios, *J. Fluid Mech.* **144,** 385–401 (1984).
12. M. J. Witte and T. A. Newell, A thermal burst model for the prediction of erosion and growth rates of a diffusive interface, ASME Paper No. 85-HT-31, ASME–AIChE Heat Transfer Conf., Denver (1985).
13. C. J. Poplawsky, F. P. Incropera and R. Viskanta, Mixed layer development in a double-diffusive, thermohaline system, *ASME J. Solar Energy Engng* **103,** 351–359 (1981).
14. J. M. Mehta, W. M. Worek and Z. Lavan, Flow-visualization studies of double diffusive convective motions in solar ponds, *Proc. Indian Sec. Int. Solar Energy Soc.*, pp. 5.029–5.035, New Delhi (1982).
15. W. T. Lewis, F. P. Incropera and R. Viskanta, Interferometric study of stable salinity gradients heated from below or cooled from above, *J. Fluid Mech.* **116,** 411–430 (1982).
16. K. A. Meyer, D. P. Grimmer and G. F. Jones, An experimental and theoretical study of salt gradient pond interface behavior, *Proc. Am. Solar Energy Soc.*, pp. 185–190, Houston (1982).
17. J. Kamal and C. E. Nielsen, Convective zone structure and zone boundaries in solar ponds, *Proc. Am. Solar Energy Soc.*, pp. 191–196, Houston (1982).
18. D. P. Grimmer, G. F. Jones, J. Tafoya and T. J. Fitzgerald, Development of a point-electrode conductivity salinometer with high spatial resolution for use in very saline solutions, *Rev. Scient. Instrum.* **54,** 1744–1748 (1983).
19. R. E. Kelley and D. Pal, Thermal convection with spatially periodic boundary conditions, resonant wavelength excitation, *J. Fluid Mech.* **86,** 433–456 (1978).
20. J. M. Mehta, Experimental and analytical investigation of a thermohaline double-diffusive system, Ph.D. dissertation, Illinois Institute of Technology, Chicago, Illinois (1985).
21. H. T. Rossby, A study of Benard convection with and without rotation, *J. Fluid Mech.* **36,** 309–335 (1969).
22. T. Y. Chu and R. J. Goldstein, Turbulent convection in a horizontal layer of water, *J. Fluid Mech.* **60,** 141–159 (1973).
23. K. B. Katsaros, W. T. Liu, J. A. Businger and J. E. Tillman, Heat transport and thermal structure in the interfacial boundary layer measured in an open tank of water in turbulent free convection, *J. Fluid Mech.* **83,** 311–335 (1977).
24. J. S. Turner, *Buoyancy Effects in Fluids*, Chap. 7. Cambridge University Press, London (1973).
25. L. N. Howard, Convection at high Rayleigh number, *Proc. 11th Int. Cong. Appl. Mech.* (Edited by H. Görtler). Springer, Berlin (1966).

26. E. M. Sparrow, R. B. Husar and R. J. Goldstein, Observations and other characteristics of thermals, *J. Fluid Mech.* **41**, 793–800 (1970).
27. M. P. Escudier and T. Maxworthy, On the motion of turbulent thermals, *J. Fluid Mech.* **61**, 541–552 (1973).
28. D. A. Nield, The thermohaline Rayleigh–Jeffreys problem, *J. Fluid Mech.* **29**, 545–558 (1967).
29. J. K. Platten and J. C. Legros, *Convection in Liquids*, Chap. IX. Springer, Berlin (1984).

MODELE PHYSIQUE DE L'EROSION DE LA ZONE GRADIENT DANS LES SYSTEMES THERMOHALINES

Résumé—On formule un modèle physique pour l'érosion de la zone gradient dans les systèmes thermohalines proches de l'équilibre. Le modèle considère les effets, aux frontières de la zone de gradient, de la modulation de la température causée par la turbulence lente dans les zones adjacentes convectives. Les équations qui gouvernent le mouvement dans une couche horizontale doublement diffusive sont résolues pour des conditions aux limites qui incorporent ces modulations. Le résultat prédit des perturbations de microconvection dans la zone de gradient, avec une amplitude qui diminue exponentiellement en s'éloignant des frontières. L'épaisseur calculée de la perturbation observable est de l'ordre de 1 cm, ce qui s'accorde avec l'observation des expériences. L'examen de la solution de la stabilité de la frontière fournit, pour la première fois, un modèle du comportement de l'érosion qui justifie une formule empirique pour l'équilibre de la frontière.

EIN PHYSIKALISCHES MODELL DES ABBAUS DER GRADIENTENZONE IN SALZLÖSUNGEN

Zusammenfassung—Ein physikalisches Modell zur Beschreibung des Abbaus der Gradientenzone in Salzlösungen nahe dem Gleichgewicht wurde aufgestellt. Das Modell beinhaltet den Einfluß von Temperaturschwankungen am Rand der Gradientenzone auf Grund von mäßig turbulenten Konvektionsströmungen in angrenzenden Bereichen. Die Gleichungen, die die Konvektionsströmungen in einem waagerechten, stabförmigen Volumen mit Temperatur- und Konzentrationsunterschieden bestimmen, werden für Randbedingungen gelöst, die diese Temperaturschwankungen beinhalten. Aus der Lösung ergeben sich Störungen durch Mikrokonvektion in der Gradientenzone, deren Amplitude exponentiell mit dem Abstand von den Randbereichen abnimmt. Die Dicke der Schicht, in der sich die Störungen beobachten lassen, beträgt etwa 1 cm, was mit tatsächlichen Beobachtungen übereinstimmt. Die Untersuchung der Stabilitätsbedingung für den Randbereich liefert zum ersten Mal ein Modell für den Abbauprozeß in der Schichtung, dessen Ergebnisse mit denen einer empirischen Gleichung für das Gleichgewicht im Randbereich übereinstimmt.

ФИЗИЧЕСКАЯ МОДЕЛЬ РАЗМЫВАНИЯ ГРАДИЕНТНОЙ ЗОНЫ В СИСТЕМАХ С ТЕРМОСОЛЕНОСТЬЮ

Аннотация—Сформулирована физическая модель размывания градиентной зоны в системах с термосоленостью вблизи усойчивого состояния. В модели учтено влияние температурных колебаний у границ градиентной зоны, вызванных слаботурбулентными восходящими потоками в соседних конвективных зонах. Уравнения, описывающие конвекцию в горизонтальной прямоугольной ячейке с бинарной диффузией решаются при граничных условиях, учитывающих колебания. Полученные результаты предсказывают микроконвективные возмущения в градиентной зоне. Их амплитуда затухает по экспоненциальному закону с удалением от границ. Предполагаемая толщина наблюдаемых возмущений порядка 1 см, что соответствует опытным данным. Анализ устойчивости границ позволил впервые получить модель размывания, согласующуюся с эмпирическим соотношением для устойчивой границы.